J Mater Sci (2011) 46:7489–7500
DOI 10.1007/s10853-011-5719-x

Viscoelastic interpretations of erosion performance of short aramid fibre reinforced vinyl ester resin composites

Sandeep Kumar · Bhabani K. Satapathy · Amar Patnaik

Received: 4 March 2011 / Accepted: 13 June 2011 / Published online: 1 July 2011

Abstract Short aramid fibre reinforced vinyl ester resin based isotropic composites are fabricated with varying fibre weight fractions (20–50 wt%). The composites were evaluated for their erosion performance under a dynamic set of variables such as impingement angle (30°–90°), impact velocity (43–76 m/s), erodent size (250–600 μm) and stand-off distance (55–85 mm) following design of experiments (DOE) based on Taguchi analysis approach. The thermo-mechanical attributes such as storage modulus, loss modulus and damping properties as viscoelastic responses of the composites were investigated in the temperature range of 0–180 °C for their possible interpretations regarding reinforcement efficiency and energy dissipation aspects relevant to erosion process. An interrelation between the full-width half-maxima (FWHM) of loss modulus peak and erosion rate has emerged indicating the erosion to be mainly controlled by the fibre–matrix interfacial characteristics. The eroded surface morphology investigation by scanning electron microscopy (SEM) revealed the nature of wear-craters, material damage mode and other qualitative attributes responsible in facilitating erosion of the composites.

Introduction

In contrast to monolithic metal alloys and ceramic materials, fibre reinforced polymer (FRP) composite materials with higher specific strength and corrosion resistances are functionally superior in their erosion performance with regard to the effect of solid particles in air/fluid stream for the integral applications of FRPs in tribo-engineering and manufacturing sectors. Component thinning, surface roughening, surface degradation, macroscopic scooping appearance and reduction in durability of the composite structures are some of the deleterious effects of solid particle erosion. Reports concerning relationship between erosion and mechanical properties of composites highlighting the interactive influences of compositional variables, viz. matrix and reinforcement type and content, experimental variables, viz. impingement angle, impact velocity, erodent type, size, shape and hardness and other inherent material attributes such as strength, ductility, crystallinity, cross-link density, reinforcement efficiency and filler/fibre distribution, etc. have critically been discussed in some of the recent literature [1–7]. Typically, erosion resistance of polymers is two or three orders of magnitude lower than that of metallic materials [4, 5, 7, 8] though erosion resistance can be enhanced by adequate reinforcement as has been reported for several thermoplastic and thermosetting resin matrix based reinforced composites [4, 9–11]. The phenomenon of wear in polymer based materials has been reported to be a consequence to adhesion, friction and several mass transfer processes that occur under various modes of tribological situations that are encountered by the materials/tribo-components [12, 13].

Pertaining to the engineering thermoplastic based materials it was reported that short E-glass fibre reinforcement improves the erosive wear resistance of polyether imide (PEI) whereas the reinforcement with glass fibre affects the wear resistance of polyphenylene sulphide (PPS) deleteriously [9, 10]. Similarly solid particle erosion behaviour of high-performance thermoplastic polymers and

S. Kumar · B. K. Satapathy (✉)
Centre for Polymer Science and Engineering, Indian Institute of Technology Delhi, Hauz Khas, New Delhi 110016, India
e-mail: bhabaniks@gmail.com; bhabani@polymers.iitd.ernet.in

A. Patnaik
Department of Mechanical Engineering, National Institute of Technology, Hamirpur 177005, Himachal Pradesh, India

their composites such as polyamides, PPS and their annealing composites have been well discussed [14–16]. Woven aramid fibre reinforced epoxy laminates in a quasi-isotropic (0/90/±45) symmetric lay-up showed larger reductions in erosion rate through the mechanistic intervention of impact-induced fibrillation of aramid fibre leading to enhanced ductility and thereby absorbing significantly more energy than the relatively brittle glass and graphite fibres based epoxy composites [8].

Regarding the material erosion performance correlations to mechanical properties, Lammy [11] found that erosion wear rate increase with increasing 'brittleness index'. Similarly, Friedrich [17] correlated the erosion resistance with hardness and fracture energy. An increase in hardness may cause an increase in brittle-erosion, whereas higher fracture energy of materials usually leads to an improvement in erosion resistance. Hutchings et al. [18] studied eight unfilled elastomers whereby a good correlation between erosive wear and rebound resilience could emerge though without much clarity concerning their relationship to glass transition or mechanical properties such as hardness, tensile strength and ultimate tensile elongation. Similarly Brandstädter et al. [19] and Böhm et al. [20] also could not establish any correlation with various mechanical properties such as modulus of elasticity, hardness and fracture energy though the former group could indicate some qualitative correlations between worn surface morphology and erosive wear. Harsha et al. [4] have reported a good linearity between steady state erosion and various mechanical properties such as $[Se]^{-1}$, $[He]^{-1}$, $[HSe]^{-1}$, $[e]^{-1}$ at 30° and 90° impingement angles for thermoplastic engineering polymer based composites. Roy et al. [5] investigated four different types of polymer matrix composites and found a correlation between erosion performance and coefficient of restitution though conventional interfacial and mechanical properties indicated the absence of any correspondence.

Vinyl ester resins (VEs) are known to be stronger than polyester resins and cheaper than epoxy resins with excellent chemical resistance, blistering resistance and impact resistance [21]. Rosario et al. [22] showed that the VE networks cured at room temperature (RT) were stronger, tougher (expected for more open network based structures), and had higher elongation than those cured at elevated temperature (140 °C). The glass transition temperature (T_g) of the networks were significantly lower with higher rubbery moduli when cured at RT confirms the openness of the VEs network structure. Thus network structures with lower cross-link density are formed when VEs were cured at lower temperature. The studies on curing and decomposition behaviour [23] and effect of degree of cure on the viscoelastic properties [24] of VE resins has also led to these inferences. Kevlar and Glass fibre reinforced vinyl ester composites were also studied for their application potential in ballistics [25]. For applications involving erosion conditions epoxy, unsaturated polyester and vinyl ester resin based long fibre and fabric reinforced composites have also been reported [8, 26–30]. Since erosion due to a single erodent/cluster of erodents is microscopically a phenomenon involving localized deformation induced progressive material damage and removal, isotropic composites such as short fibre reinforced thermosets would theoretically be superior. In this context epoxy based thermosetting composites have already been evaluated filled with particulates such as red-mud, fly-ash and fibres such as short glass fibres and natural fibres like bamboo/bagasse fibres [28–31]. However, toughened composites such as short aramid fibre reinforced vinyl ester resin composites with enhanced viscoelastic performance have not yet been evaluated for their erosion performance, an investigation of key significance for exploring them as composites for industrial and structural components that are exposed.

The present paper deals with the comprehensive assessment of short aramid fibre reinforced vinyl ester resin composites for their dynamic mechanical properties as a measure of their viscoelastic responses and its possible interrelation to erosion performance vis-à-vis parametric optimization to attain a novel composite design ideology for enhanced wear resistance.

Experimental

Preparation of composites

Short aramid fibres (density: 1.44 g/cm^3) (Teijin) of 6 mm length are mixed in vinyl ester (VE) resin (density: 1.05 g/cm^3) (Ciba–Geigy) to prepare the composites at a temperature of 30 °C compressed under 10 kg/cm^2 for 24 h. The curing of vinyl ester resin is done by incorporation of 2% methyl ethyl ketone peroxide (MEKP) catalyst and 0.3% cobalt naphthenate (accelerator) along with 0.05% of 2,4-pentanedione (retarder for the extension of the reaction gel time) by weight. The matrix has Barcol hardness, tensile modulus and tensile strength of 40, 2.6–3.4 GPa and 65 MPa, respectively. The flexural modulus and strength are about 3.6 GPa and 125 MPa, respectively. The heat distortion temperature is 105 °C. The details of composite designation and composition are given in Table 1.

Dynamic mechanical properties of the composites

The viscoelastic responses of the composites were measured using dynamic mechanical analysis (DMA) and conducted in a nitrogen atmosphere at a fixed frequency of 1 Hz, heating rate of 5 °C/min, temperature range of 0–180 °C and at a strain of 1% on rectangular samples with

Table 1 Details of composite designation and composition

Composite designation	Composition (wt% fraction)	
	Vinyl ester resin	Aramid fibre
VAF0	100	00
VAF20	80	20
VAF30	70	30
VAF40	60	40
VAF50	50	50

approximate dimensions of 38 × 12.5 × 3.5 mm using a TA instruments-Q800 model DMA instrument in bending mode [32, 33].

Evaluation of erosive wear performance

The erosion experiments are carried out on samples of 30 mm×30 mm with 0.5 mm thickness as per ASTM G76 on an erosive wear test rig, whose details are reported elsewhere [33]. In this study, dry silica sand (pyramidal shaped) of different particle sizes (250, 355, 420 and 600 μm) are used as erodent. The mass losses due to erosion are calculated and erosion rates were determined. The erosive wear performance were determined following the Taguchi's technique as a multi-parametric optimization model since the erosive wear is functionally dependent on multiple experimental variables such as impact velocity (factor A), fibre loading (factor B), impingement angle (factor C), stand-off distance (factor D), erodent size (factor E) and their simultaneous interactions. Using Taguchi's technique (a) firstly the control factors have been identified and (b) subsequently steady state erosion characteristics of the composites were determined up to three selected level of optimally controlled operating variables. The implementation of design of experiment (DOE) and the analysis of the outputs following the Taguchi technique was carried out by using the software MINITAB 14 which is reported elsewhere [34]. For the present investigation L_{16} (4^5) orthogonal arrays were selected depicting the effect of five parameters-four level factors. The static and the dynamic variables chosen for the test are given in Tables 2 and 3. Conforming to the Taguchi approach, the details of the control factors following DOE are assigned to particular columns of the L_{16} (4^5) inner orthogonal array which are given in Table 4. The S/N analysis (S/N: signal-to-noise ratio) is calculated to analyze experimental results, where the performance ideology of smaller-the-better norm for S/N ratio is adopted. The S/N may be given as below.

$$\text{S/N} = -10\log(\text{M.S.D.})$$

where M.S.D. is the mean-square deviation for the output characteristic, i.e. erosive wear rate. To obtain optimal performance, lower-the-better characteristic for erosion rate must be taken. The mean-square deviation (M.S.D.) for the lower-the-better characteristic may be expressed as below [34].

$$\text{M.S.D.} = \frac{1}{m}\sum_{i=1}^{m} T_i^2 \quad (1)$$

where m is the number of tests and T_i is the value of experimental result of the ith test.

Furthermore, a statistical analysis of variance (ANOVA) is performed to identify the influencing parameters that are

Table 2 Parameters of the setting

Control factors	Symbols	Fixed parameters	
Velocity of impact	Factor A	Erodent	Silica sand
Fibre loading	Factor B	Erodent feed rate (g/min)	10.0 ± 1.0
Impingement angle	Factor C	Nozzle diameter (mm)	3
Stand-off distance	Factor D	Length of nozzle (mm)	80
Erodent size	Factor E		

Table 3 Levels for various control factors

Control factor	Level				
	I	II	III	IV	Units
A: Velocity of impact	43	54	65	76	m/s
B: Fibre loading	20	30	40	50	%
C: Impingement angle	30	45	60	90	°C
D: Stand-off distance	55	65	75	85	(°)
E: Erodent size	250	355	420	600	μm

Table 4 Experimental design using L_{16} orthogonal array

Expt. no.	A (m/s)	B (%)	C (°)	D (mm)	E (μm)	E_r (10^{-4} g/g)	S/N ratio (dB)
1	43	20	30	55	250	1.416667	76.9746
2	43	30	45	65	355	0.75000	82.4988
3	43	40	60	75	420	1.833333	74.7352
4	43	50	90	85	600	4.250000	67.4322
5	54	20	45	75	600	3.875000	68.2346
6	54	30	30	85	420	0.937500	80.5606
7	54	40	90	55	355	0.062500	84.0824
8	54	50	60	65	250	0.812500	81.8035
9	65	20	60	85	355	9.421053	60.5180
10	65	30	90	75	250	1.263158	77.9708
11	65	40	30	65	600	3.105263	70.1580
12	65	50	45	55	420	1.684211	75.4721
13	76	20	90	65	420	1.857143	74.6231
14	76	30	60	55	600	9.047619	60.8693
15	76	40	45	85	250	3.142857	70.0535
16	76	50	30	75	355	6.761905	63.3986

statistically significant. With the S/N and ANOVA analyses, the optimal combination of the influencing parameters can be predicted to a useful level of accuracy. Finally, a confirmation experiment is conducted to verify the optimal control variables obtained from the parametric DOE.

The evaluation of erosive wear performance at different variable levels is carried out by the steady state erosive wear rate determination at the optimized parameter levels obtained Taguchi-DOE technique. The ratio of the weight loss to the weight of the eroding particles causing the loss is then computed as a dimensionless incremental erosion rate.

Worn surface morphology

The erosion mechanisms of aramid fibre reinforced vinyl ester resin composites materials were investigated by scanning electron microscopy (SEM) of the worn surface using ZEISS EVO Series Scanning Electron Microscope Model EVO 50. The impact and other erosion parameters induced craters and material deformation and damage modes have been qualitatively assessed.

Results and discussion

Dynamic mechanical properties of composites

The viscoelastic responses of the composites in the entire range of fibre loadings have been obtained by conducting DMA to investigate the variation of storage modulus (E'), loss modulus (E'') and damping parameter (tan δ) as a function of temperature as shown in Figs. 1, 2, and 3. The Cole–Cole plots for the composites are shown in Fig. 4.

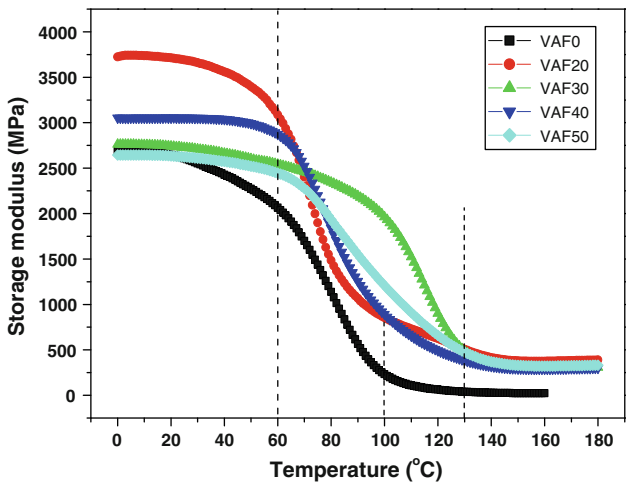

Fig. 1 Variation of the storage modulus (E') as a function of temperature

Viscoelastic storage modulus

The variation of storage modulus (E') as a measure of the energy stored due to elastic deformation of the composites has shown three distinct regimes, viz., glassy regime in the range of ~0–60 °C, glassy-to-rubber transition regime characterized by a substantial decay of E' in the range of ~60–100 °C and the rubbery regime indicating degradation in the moduli above ~100–130 °C (Fig. 1). Further it has been observed that at a temperature of <60 °C the storage moduli followed the trend as

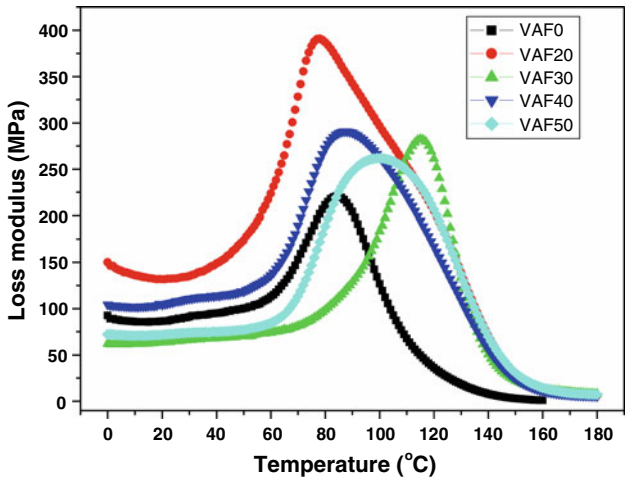

Fig. 2 Variation of the loss modulus (E'') as a function of temperature

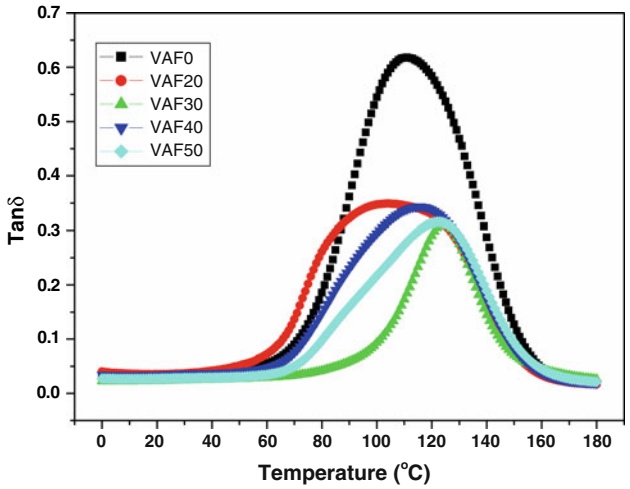

Fig. 3 Variation of the damping parameter (tan δ) as a function of temperature

$E'_{VAF20} > E'_{VAF40} > E'_{VAF30} > E'_{VAF50} > E'_{VAF0}$. This was closely followed by a distinct modulus decay regime in the range of ~60–100 °C for the unfilled vinyl ester resin matrix beyond which the rubbery/degradation regime ensued. The onset-temperature for E'-decay of the composites is found to be in the order VAF30 > VAF50 > VAF40 > VAF20 > VAF0. However, for the aramid fibre reinforced vinyl ester composites the rubbery regime undergoes a shift from ~100 °C (for the neat matrix) to ~130 °C. Interestingly, for the composite VAF30 the glassy regime has been observed to be substantially extended to a temperature of ~100 °C, which is the temperature at which the rubbery regime for neat vinyl ester resin matrix starts. However, such an extended glassy regime has also been observed to be adequately complemented by a shortened E'-decay (glassy-rubbery transition)

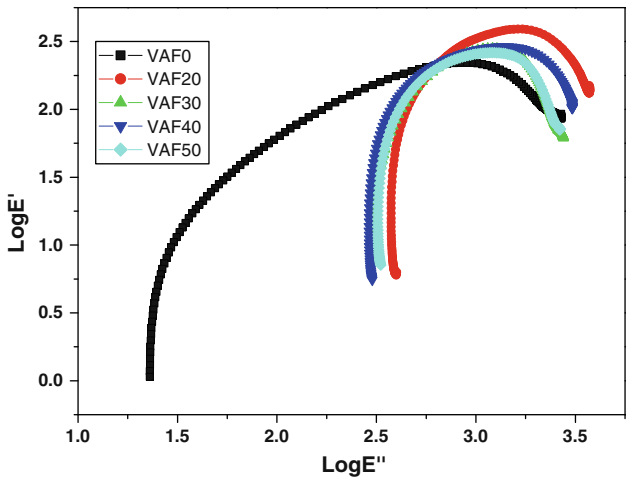

Fig. 4 Cole–Cole plot of aramid fibre vinylester composites at different fibre loading

regime. Inevitably such an observation indicates that the glass-rubbery transition regime/rubbery regime is extended by an excess of ~30 °C due to the incorporation of 30 wt% of short aramid fibre in contrast to the temperature at which the rubbery regime sets in for the neat vinyl ester matrix, i.e. ~100 °C. Such glassy regime extension to higher temperatures (from ~60 °C in matrix to ~100 °C in VAF30) vis-à-vis rubbery regime shortening may be attributed to the additional energy storage mechanism via efficient stress-transfer mechanism across the fibre–matrix interface during elastic deformation of the composite VAF30.

Viscoelastic loss and dissipation

The loss modulus (E'') representing the non-recoverable vibrational energy is shown in Fig. 2. It was observed that with the increase in the fibre content the E'' versus temperature spreads across a wider temperature range leading to an increase in the peak-width. Such effects have been attributed to the consequences of inhibition of the chain segmental relaxation process. The inhibition of the chain segment relaxation is due to an increase in the overall rigidity of the composites consequent upon the enhanced degree of material heterogeneity. The increase in peak height has been reported to be an indicator of poor interface via enhanced chain mobility whereas good interfacial adhesion may be characterized by a lower loss-peak height [35]. Further it has also been observed that for the composites with lower fibre content the shift in the loss-peak is more towards higher temperature. The composites showing narrow half-peak-width/full-width half-maxima (FWHM) may be correlated to a better relaxation mechanism operating in the polymer composite. The broadening of the loss-peaks was attributed to increase in fibre content.

Theoretically, narrow/sharp loss-peaks with lower E'' value have been reported to be due to low cross-link density whereas a broader loss-peaks with shorter loss-peak height may indicate a high cross-link density [36].

The variation of damping factor (tan δ) of the VE and its composites as a function of temperature is shown in Fig. 3. Characteristically tan δ is a measure of the mechanical damping or internal friction in a viscoelastic system. A higher tan δ value is indicative of a material that has a high non-elastic strain component, while a lower value indicates one that is more elastic. The tan δ (ratio of the loss modulus to storage modulus E''/E') was very high for the neat resin due to high reduction of the storage modulus values on rising the temperature. Incorporation of the fibres restricted the mobility of the resin molecules, raised the storage modulus values and reduced the viscoelastic lag between the stress and the strain and hence, the tan δ values were lower in the composites [37] indicating lowered damping capacity of composites. The tan δ value was decreased in the composites compared to neat resin also because there was less-matrix by volume to dissipate the vibrational energy [38]. However, there was no change in tan δ above 120 °C irrespective of the fibre weight fraction in the composites (Fig. 3).

Cole–Cole plot

The Cole–Cole plot analysis has been carried out and is shown in Fig. 4. The nature of the Cole–Cole plot indicates the homogeneity of a composite system [39]. The homogeneous system typically exhibits a semi-circular curve [32]. Interestingly the investigated short aramid fibre reinforced vinyl ester resin composites have shown curvatures as imperfect semicircles indicating that the composites are heterogeneous in nature. Additionally the apparent nature of the curvature obtained in the Cole–Cole plot also indicates a better fibre–matrix adhesion. The composites VAF30 and VAF50 have shown better interfacial characteristics than the other two composites.

Erosive wear performance of composites

Composites response optimization for influencing variables

The S/N response (signal-to-noise ratio) for erosion rate is mentioned in Table 4 and the overall mean for the S/N ratio of erosion rate is found to be 73.08 dB. In the main effect of control factors on wear rate plot if the line for a particular factor is near horizontal, then the factor has no significant effect. On the other hand, a factor for which the line has the highest inclination will have the most significant effect. It is very much clear from Fig. 5 that factors A_2, B_2, C_4, D_2 and E_1 have been observed to be significantly influential with regard to the effects derived on the basis of smaller-the-better norm.

ANOVA and the effects of factors

In order to find out the statistical significance of various factors like impact velocity (A), fibre loading (B), impingement angle (C), stand-off distance (D) and erodent

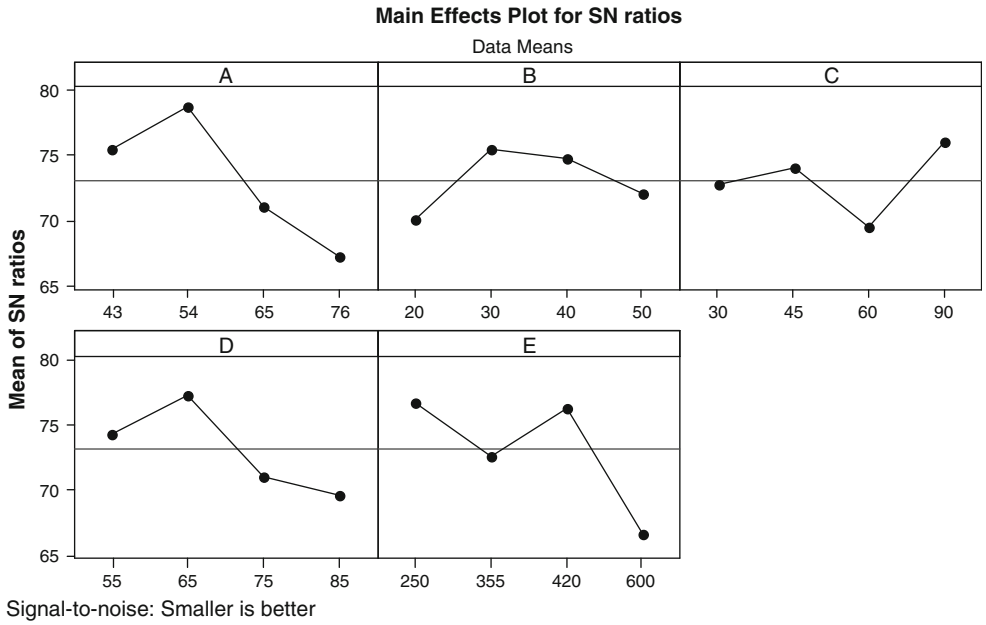

Fig. 5 Effect of control factors on erosion rate

Table 5 ANOVA table for erosion rate

Source	DF	Seq SS	Adj SS	Adj MS	*F*	*p*
A	3	206.89	206.89	206.89	5.59	0.040
B	3	5.20	5.20	5.20	0.14	0.716
C	3	13.98	13.98	13.98	0.38	0.553
D	3	82.51	82.51	82.51	2.23	0.166
E	3	186.70	186.70	186.70	5.04	0.049
Error	0	370.18	370.18	37.02		
Total	15	865.46				

size (E) on erosion rate, ANOVA is performed on experimental data. Table 5 shows the results of the ANOVA with the erosion rate. This analysis is undertaken for a level of confidence of significance of 95%. The last column of the table indicates that the main effects are highly significant (all have very small p values) [40].

From Table 5, one can observe that impact velocity ($p = 0.040$), erodent size ($p = 0.049$), stand-off distance ($p = 0.166$) and impingement angle ($p = 0.533$) have great influence on wear rate but fibre loading ($p = 0.716$) has less significant contribution on erosion rate.

Confirmation experiment

Apart from the determination of the optimal combination of control factors to minimize wear a confirmation experiment has also been performed by taking an arbitrary set of factor combination $A_3B_4C_2D_4E_3$ on erosion rate (Table 6). The estimated S/N ratio for wear rates can be calculated using the predictive equation:

$$\bar{\eta}_1 = \bar{T} + (\bar{A}_3 - \bar{T}) + (\bar{B}_4 - \bar{T}) + (\bar{C}_2 - \bar{T}) + (\bar{D}_4 - \bar{T}) + (\bar{E}_3 - \bar{T}) \quad (2)$$

where $\bar{\eta}_1$ predicted average, $\bar{T}$ overall experimental average, $\bar{A}_3, \bar{B}_4, \bar{C}_2, \bar{D}_4$ and $\bar{E}_3$ mean response for factors at designated levels. By combining like-terms, the equation reduces to

$$\bar{\eta}_1 = \bar{A}_3 + \bar{B}_4 + \bar{C}_2 + \bar{D}_4 + \bar{E}_3 - 4\bar{T} \quad (3)$$

A new combination of factor levels A_3, B_4, C_2, D_4 and E_3 is used to predict wear rate through prediction equation and it is found to be $\bar{\eta}_1 = 70.7635$ dB.

For each performance measure, an experiment is conducted for a different factors combination and compared with the result obtained from the predictive equation as shown in Table 6. The confirmation experiments lead to the conclusion that the predictive equation gives rise to wear rates of reasonable level of accuracy. An error of 6.36% for the S/N ratio of wear rate is observed, which however, may further be reduced by increasing the number of experiments. The proximity of the predicted wear to that of the experimental wear with reasonable level of accuracy essentially validates the mathematical model for wear performance prediction based on knowledge of the input (experimental) parameters.

Steady state erosion rate

Among numerous factors influencing the erosion wear of materials, the most important are impact velocity, impingement angle and particle size. The quantification of the extent of the erosion induced damage is typically ascertained by erosion rate that is expressed as the weight of material removed by unit weight of impacting particles.

Influence of impingement angle

Impingement angle is one of the most important parameters in erosion behaviour. The influence of impingement angle on the steady state erosion rate of short aramid fibre reinforced vinyl ester resin composites at a constant impact velocity of (54 m/s), erodent size of 355 μm and stand-off distance of 65 mm is shown in Fig. 6. It can be seen that steady state erosion rate is maximum at 60° impingement angle for the neat vinyl ester resin whereas remained nearly

Table 6 Results of the confirmation experiments for erosion rate

	Optimal control parameters	
	Prediction	Experimental
Level	$A_3B_4C_2D_4E_3$	$A_3B_4C_2D_4E_3$
S/N ratio for erosion rate (dB)	70.7635	66.2629

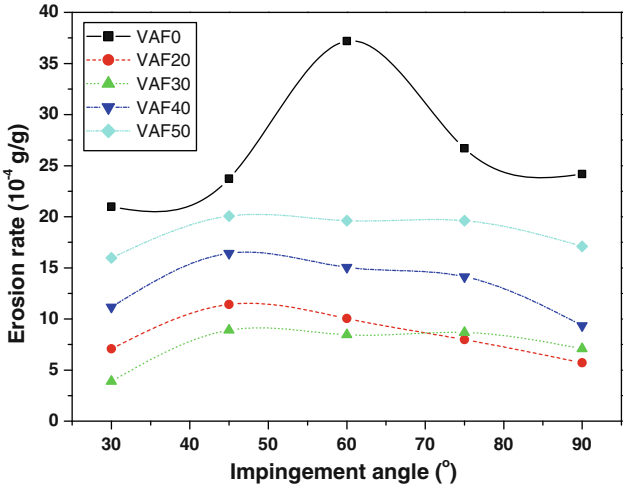

Fig. 6 Effect of impingement angle on the erosion wear rate of the composites (at constant impact velocity: 54 m/s, stand-off distance: 65 mm and erodent size: 355 μm)

unaffected in the case of the composites irrespective of the weight fraction of aramid fibre. This may be attributed to the random orientation of the short aramid fibres, i.e. more isotropic nature of the composite. Materials may broadly be classified as ductile or brittle, based on the dependence of their erosion rate with impingement angle. The ductile behaviour is typically characterized by maximum erosion rate at low impingement angle ($15° < \alpha < 30°$). On the other hand, if the maximum erosion rate occurs at normal impact ($\alpha = 90°$), the behaviour of material is brittle. Reinforced composites have been found to exhibit semi-ductile behaviour with the maximum erosion rate at intermediate impingement angles, typically $45° < \alpha < 60°$ [5, 27, 41]. However, the dependence of erosive wear behaviour on the experimental conditions and the composition of the target material were critically argued by Barkoula and Karger-Kocsis [42]. The neat vinyl ester resin, a relatively brittle matrix (compared to the nature of the fibre) showing a peak erosion rate at 60° impingement angle apparently indicates that the matrix resin is more semi-ductile rather than brittle. In case of the aramid fibre reinforced composites, not only the erosion peak apparently shifts to lower value of impingement angle (i.e. 45°) indicating enhanced ductility of the composites due to reinforcement but also the erosion resistance of composites is increased significantly with increase in short aramid fibre content. Composite having 30 wt% short aramid fibre loading showed the best erosion resistance as compared to other investigated composites whereas the composite with 50 wt% aramid fibre loading remained least wear resistant. The overall trend of erosive wear resistance was 30 wt% > 20 wt% > 40 wt% > 50 wt% of aramid fibre content in decreasing order. The matrix resin remained most susceptible to impingement angle. This inevitably indicates that an optimum resin-to-fibre content ratio functionally critical for erosive wear performance enhancement. To further understand the non-linear wear performance dependence on the weight fraction of such fibres the worn surface analysis were carried out on the eroded surfaces using SEM and is discussed in a subsequent section.

Influence of impact velocity

In order to study the effect of impact velocity on erosion rate, erosion tests are performed on the composites by varying the impact velocity from 43 to 76 m/s while impingement angle (60°), stand-off distance (65 mm) and erodent size (355 μm) were kept constant. The steady state erosion wear rates of the composites systematically increased with the increase in the impact velocity, an observation consistent with the theoretical expectations, as seen in Fig. 7. Due to an overall increase in the kinetic energy of the sand particles, with the increase in impact velocity of the erodents, which are hitting the composite targets an increased impingement-effect, may be observed leading to enhanced wear. It was observed that the composite with 30 wt% of aramid fibre is most resistant to erosion followed by the composites with 20, 50 and 40 wt% fibre contents in decreasing order. The neat vinyl ester resin remained most vulnerable to erosion damage as evident from the constantly increasing trend with much higher magnitude of erosion rate with impact velocity. Further it has also been observed that the extent of erosion susceptibility to impact velocity was much lesser than the impingement angle. However, their underlying mechanistic aspects involving generation of micro-cracks, coalescence of the micro-cracks, wear-generation, subsurface

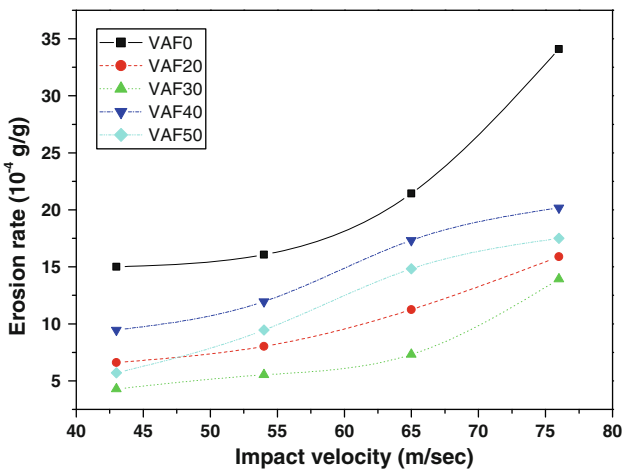

Fig. 7 Effect of impact velocity on the erosion wear rate of the composites (at constant impingement angle: 60°, stand-off distance: 65 mm and erodent size: 355 μm)

damage and wear crater characteristics may need further investigation.

Influence of erodent size

The erosion rate has been observed to be increased by varying erodent size from 250 to 600 μm at constant impact velocity (54 m/s), impingement angle (60°) and stand-off distance (65 mm) as shown in Fig. 8. On increasing the erodent size from 250 to 350 μm the erosion rate remained relatively unaffected. In contrast the erosion rate increased appreciably on further increasing the erodent size from 350 to 420 μm and subsequently to 600 μm. The maximum erosion rate is observed irrespective of the fibre content for the erodents with a particle size of 600 μm. Such non-uniform trend of erosion rate enhancement, from size considerations point of view, may be attributed to the fact that at sufficiently large particle sizes of the erodent the surface roughness (in terms of sharp edges promoting indentation efficiency) and the area of the impact zone on the composite may get substantially increased. As a consequence of such increases in surface roughness of erodent vis-à-vis indentation impact zone a larger amount of material removal/selective dislodging of the phases (matrix and reinforcement) may take place giving rise to enhanced erosion rate. The dependence of erosion rate on the erodent size has already been discussed in our previous paper, where the interplay of momentum of the erodent, indentation efficiency and fatigue assisted erosive wear modes play crucial roles from material mechanics point of view [33]. It should also be mentioned that the composite with 30 wt% of aramid fibre content remained most erosion resistant closely followed by the composite with 50, 40 and 20 wt% of aramid fibre content.

Viscoelastic correlations to erosive performance

The steady state erosion performance assessment as a function of impingement angle, impact velocity and erodent sizes has revealed that the erosive wear rate minimization of short aramid fibre reinforced vinyl ester resin composites may be accomplished by resorting to an impingement angle of 45°, impact velocity of 54 m/s, erodent size of 355 μm and fibre content of 30 wt% (VAF30) in the composite. Such an optimization of the composites for wear minimization may also be evident from the viscoelastic loss behaviour related correlation plot showing erosive wear rate versus FWHM of the loss modulus (E'') peak and brittleness (B) as a function of fibre concentration (Fig. 9). The correlation plot revealed a striking resemblance in the trend of the erosion performance (especially for impingement angle) and FWHM dependence of the fibre content irrespective of the optimum impingement angle, impact velocity and erodent size. Theoretically a lower FWHM value corresponding to loss modulus peak indicates a better relaxation behaviour [35, 43]. Fundamentally the correspondence between FWHM and the homogeneity of amorphous phase is well understood. Qualitatively, smaller FWHM implies a larger relaxation time distribution of the network involved and thereby it leads to a higher inhomogeneity of the amorphous phase, an aspect which is also evident from the nature of the Cole–Cole plot [32, 39]. Thus a broader loss modulus peak

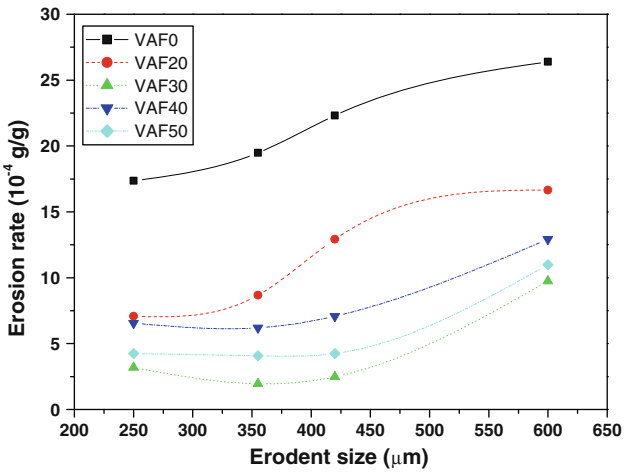

Fig. 8 Effect of erodent size on the erosion wear rate of the composites (at constant impact velocity: 54 m/s, impingement angle: 60° and stand-off distance: 65 mm)

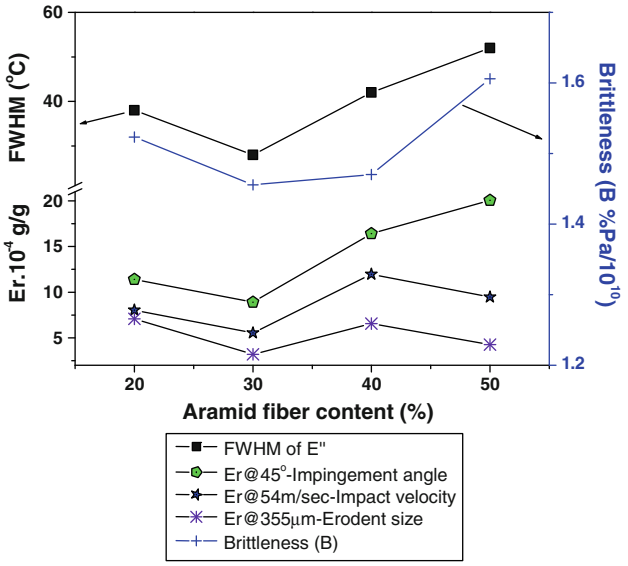

Fig. 9 Correlation of erosion rate (E_r) with brittleness and full-width half-maxima (FWHM) of loss modulus of aramid fibre reinforced vinyl ester composites

with larger inhomogeneity of the amorphous phase characterized by the parameter FWHM has a direct bearing on the erosion process, revealing a fundamental interrelationship between loss-behaviour that is more heterogeneous leading to a better relaxation response with enhanced interfacial adhesion/reinforcement efficiency of the composites and erosion performance. The brittleness (B) at any given temperature (T) may be calculated according to the equation; $B = (\varepsilon_b E')^{-1}$, where ε_b is the elongation at break in tensile testing mode and E' is the storage modulus of the materials at RT (30 °C). The variation of brittleness parameter B with erosion rate is shown in Fig. 9. The physical significance of B lies in its correspondence to the dimensional stability of the material in service subjected to repetitive loading [44, 45]. From Fig. 9 it was observed that a lower the B-value may lead to higher stability as in 30% filled aramid short fibre reinforced vinyl ester composites. Despite such broad correspondence between brittleness and erosion stability a greater deviation at higher fibre loading (40–50 wt%) has been observed in contrast to the correlation between erosion and FWHM. Such deviations in trends may be attributed to the loss of the self-similarity of resulting erosion rate curves of FRPs. Brittleness is typically evaluated for the thermoplastic polymeric materials and reportedly has an exponential correlation with the sliding wear/extent of modulus recovery [46, 47]. For example, EPDM/PP based thermoplastic vulcanizate (TPV) modified and unmodified materials with ceramic inclusions/fillers and coupling agents have been reported to be exhibiting low brittleness compared to ceramic based PP materials [47]. Similarly higher strain at break and low brittleness (e.g. 40 wt% fibre filled composite) may be an effect that was considered akin to plasticization provided by the unreacted styrene or other chemicals used for curing of VE resin.

Worn surface morphology

To verify the erosion mechanisms of aramid fibre reinforced vinyl ester resin composite materials, eroded surfaces of the composites are observed under different impingement angles by SEM. Figure 10 shows the SEM micrographs of aramid fibre reinforced composite eroded at impingement angles of 30°, 45°, 60° and 90°. Not only at the lower but also at the higher impingement angles, both the ductile damage and the brittle cracks were viewed simultaneously. In the case of the impingement angle of 30° (a) (see Table 4, Experiment 1) and 90° (b) (see Table 4, Experiment 7) as shown in Fig. 10a, b for 20 wt% fibre loading, the characteristics of the ductile material are apparent. In particular, at 90°, the fibre damage resulting from recurring micro-ploughing in combination with the fibres getting slowly worn out from the matrix surfaces were observed. The experimental erosion rate of such composites at 90° is lower than that at 30° suggesting that the ductile damage is maintained at an impact angle of 90°, and that it could prevent the fibre fractions from being removed from the materials. In the case of the impingement angle of 45° for the same composite, the cracks seemed to extend quickly, causing the fibre bunch to fracture together as shown in Fig. 10c (see Table 4, Experiment 5).

Therefore, the removed fibre fragments are much larger than with other angles. On the other hand on further increasing the fibre loading (i.e. 30 wt%) the micrograph (Fig. 10d) shows a similar trend as seen in Fig. 10c with lower impact velocity (43 m/s), lower stand-off distance (65 mm) and lower erodent size (355 μm), that cause material removal only by microcutting and/or microploughing (see Table 4, Experiment 2). As compared to Fig. 10d at an impact velocity of 45 m/s to that at 54 m/s in Fig. 10e (with lower impingement angle (30°)) mainly resin removal (in the early stages of erodent hits) that expose the fibres to breakage and (in the later stages) fibre breakage without subsequent fibre removal are observed (see Table 4, Experiment 6). Further continuation of erosion by sand particle impacts resulted into fibre–matrix interfacial damage. This damage is characterized by the separation and detachment of broken fibres from the resin matrix, as shown in Fig. 10f. The observed behaviour of these materials can be attributed to the following mechanism. It is well known that the fibres in composites subjected to particle flow, undergo breakage when subjected to bending. Thus, local removal of resin material from impacted surface, which results in the exposure of the fibres (see Table 4, Experiment 11) may be conjectured. Such effects cause intensive debonding and breakage of the fibres, which are not supported by the matrix.

The observed erosion damage is characterized by exposure of aramid fibres, fibre–matrix debonding, multiple fibre cracking and material removal. Plastic deformation, melting of matrix, pit formation and dislodging of fibre are also seen on the surface of the investigated polymeric composites. The impingement of the erodent caused roughening of the surface of the material, especially in higher contact angles. A characteristic feature of more cutting with chip formation is reflected (Fig. 10e, f). Erosion along the fibres and clean removal of the matrix to expose aramid fibres is also seen (Fig. 10f). The matrix shows multiple fractures and material removal.

The exposed fibres are broken into fragments and thus can be easily removed from the worn surfaces. Figure 10g shows the SEM micrographs of surface features in aramid fibre (40 wt%) reinforced vinyl ester resin composites (VAF40) eroded at impingement angles of 90°. Interestingly both the

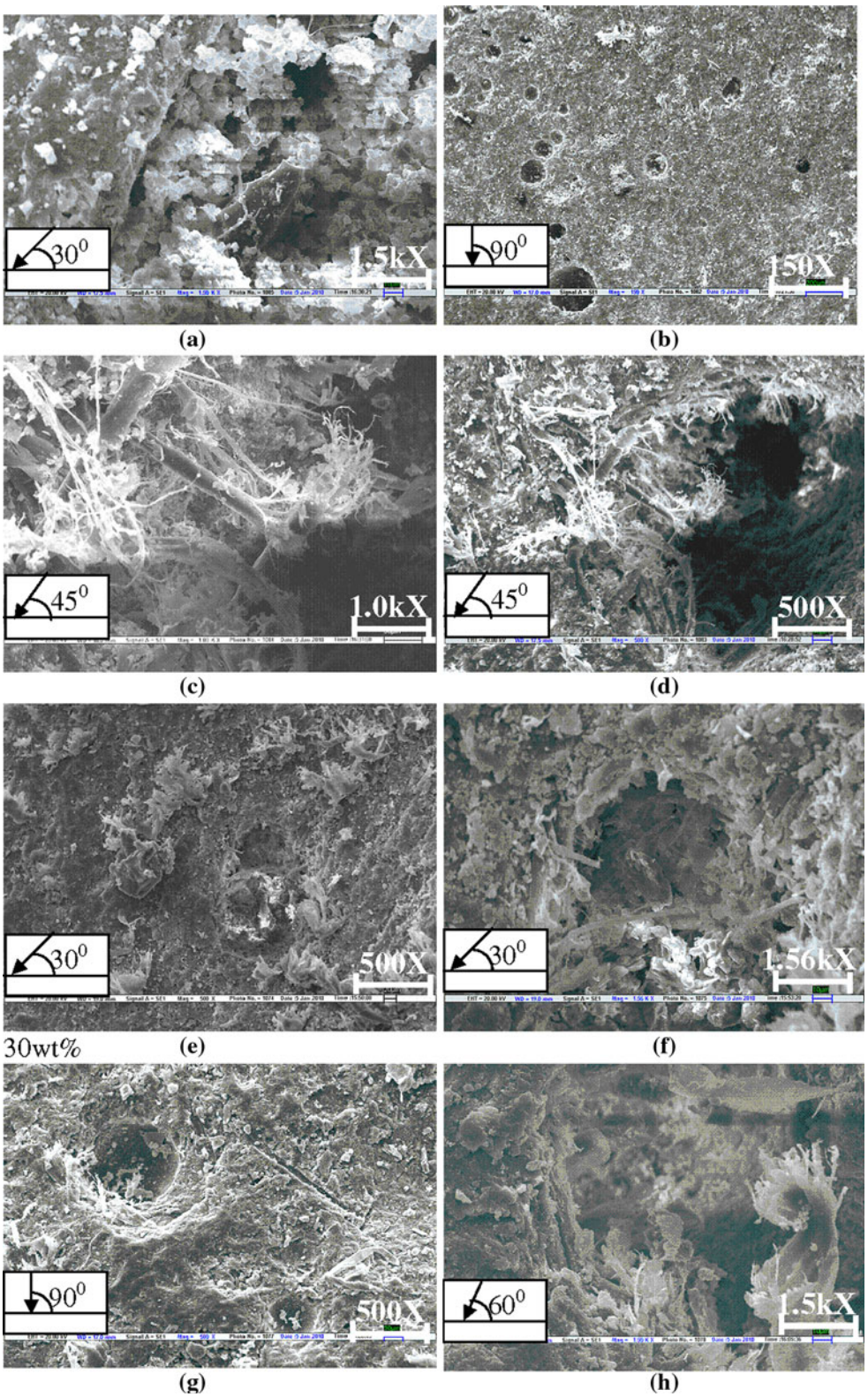

Fig. 10 SEM micrograph of aramid fibre reinforced vinyl ester resin composites

ductile damage and the brittle cracks are viewed simultaneously not only at the lower but also at the higher impingement angles (see Table 4, Experiment 7). It is indicated from Fig. 10h that damage processes of the composite is only on the surface without any broken-off fibres (see Table 4, Experiment 3).

Conclusions

Parametric optimization of the influencing material-variables (resin-to-fibre content ratio) and experimental variables (stand-off distance, impingement angle, erodent size, impact velocity, etc.) for erosion resistance maximization/erosive wear performance enhancement of short aramid fibre reinforced vinyl ester resin composites has been successfully attempted following DOE approach based on Taguchi optimization technique. The viscoelastic response of the composites, the extent of relaxation, vis-à-vis inhomogeneity aspects with respect to the amorphous content has been critically investigated. It was estimated from optimization that the material and experimental variable combination with an impact velocity of 43 m/s, aramid fibre loading of 30 wt% in the composite, impingement angle of 60°, a stand-off distance of 85 mm and erodent size of 420 μm may potentially lead to an optimum erosive wear performance. The peak erosion rate shifts to a larger value of impingement angle compared to the ductile materials and due to the ductile nature of the aramid fibre the composites exhibited a maximum erosion rate at an impingement angle of 45° under the present experimental conditions for four different fibre loading and at constant impact velocity of 54 m/s. The composite with 30 wt% of short aramid fibre content has been observed to be most resistant to erosion damages under a fixed set of optimized experimental variables, i.e. in the steady state erosion mode. The visco-elastic correlations to erosion performance in terms of a correspondence between erosion and FWHM of loss modulus and brittleness curve has been established, indicating the relaxation dynamics of the short aramid fibre reinforced vinyl ester resin composites to be the major determinant of erosion performance. Thus our study demonstrates the fact that erosion behaviour of short fibre reinforced vinyl ester composites is interface-controlled like the mechanical damage aspects of the composites under static and dynamic stress situations.

References

1. Patnaik A, Satapathy A, Chand N, Barkoula NM, Biswas S (2010) Wear 268:249
2. Biswas S, Satapathy A, Patnaik A (2010) J Reinf Plast Compos 29:2898
3. Barkoula NM, Karger-Kocsis J (2002) J Mater Sci 37:3807. doi:10.1023/A:1019633515481
4. Harsha AP, Tewari US, Venkataraman B (2003) Wear 254:693
5. Roy M, Vishwanathan B, Sundararajan G (1994) Wear 171:149
6. Häger A, Friedrich K, Dzenis YA, Paipetis SA (1995) In: Street K, Whistler BC (ed) ICCM-10 conference proceedings, Canada. Woodhead Publishing, Cambridge, p 155
7. Tilly GP, Sage W (1970) Wear 16:447
8. Pool KV, Dharan CKL, Finne I (1986) Wear 107:1
9. Harsha AP, Thakre AA (2007) Wear 262:807
10. Suresh A, Harsha AP, Ghosh MK (2009) Wear 266:184
11. Lammy B (1984) Tribol Int 17:35
12. Myshkin NK, Petrokovets MI, Kovalev AV (2005) Tribol Int 38:910
13. Brostow W, Deborde J-L, Jaklewicz M, Olszynski P (2003) J Mater Edu 24:119
14. Rajesh JJ, Bijwe J, Venkataraman B, Tiwari US (2002) J Mater Sci 37:5107. doi:10.1023/A:1021012404839
15. Yilmaz T (2010) J Mater Sci 45:2381. doi:10.1007/s10853-009-4204-2
16. Arjula S, Harsha AP, Ghosh MK (2008) J Mater Sci 43:1757. doi:10.1007/s10853-007-2405-0
17. Friedrich K (1986) J Mater Sci 21:3317. doi:10.1007/BF00553375
18. Hutchings IM, Deuchar DWT, Muhr AH (1987) J Mater Sci 22:4071. doi:10.1007/BF01133360
19. Brandstädter A, Goretta KC, Routbort JL, Groppi DP, Karasek KR (1991) Wear 147:155
20. Böhm H, Betz S, Ball A (1990) Tribol Int 23:399
21. Suresha B, Chandramohan G (2008) J Mater Process Technol 200:306
22. Rosario AC, Burts-Cooper E, Riffle JS (2007) Polymer 481:203
23. Gaur B, Rai JSP (1992) Polymer 33:4210
24. Scott FT, Cook DW, Forsythe SJ (2008) Eur Polym J 44:3200
25. Panda SP, Naval NG, Saraf MN, Gupta RK, Goel RA (1994) Def Sci J 44:341
26. Mathew MT, Padaki Naveen V, Rocha LA, Gomes JR, Alagirusamy R, Deopura BL, Frangueiro (2007) Wear 263:930
27. Tewari US, Harsha AP, Häger AM, Friedrich K (2003) Compos Sci Technol 63:549
28. Srivastava VK, Pawar AG (2006) Compos Sci Technol 66:3021
29. Biswas S, Satapathy A (2010) Mater Des 31:1752
30. Yilmaz MG, Unal H, Mimaroglu A (2008) Express Polym Lett 2:890
31. Mishra P, Acharya SK (2010) Int J Phys Sci 5:109
32. Menard KP (2008) Dynamic mechanical analysis: a practical approach. Taylor & Francis, New York
33. Kumar S, Satapathy BK, Patnaik A (2011) Mater Des 32:2260
34. Glen SP (1993) Taguchi methods: a hands-on approach. Addison-Wesley, New York
35. Ornaghi HL, Bolner AS, Fiorio R, Zattera AJ, Amico SC (2010) J Appl Polym Sci 118:887
36. John JLS, Matthew SL, James MS, Giuseppe RP (2008) Compos Sci Technol 68:1869
37. Ghosh P, Bose NR, Mitra BC, Das S (1997) J Appl Polym Sci 62:2467
38. Ray D, Sarkar BK, Das S, Rana AK (2002) Compos Sci Technol 62:911
39. Idicula M, Malhotra SK, Joseph K, Thomas S (2005) Compos Sci Technol 65:1077
40. Montgomery DC (2005) Design and analysis of experiments, 5th edn. Wiley, New York, p 363
41. Kulkarni SM, Kishore K (2001) Polym Compos 9:25
42. Barkoula NM, Karger-Kocsis J (2002) Wear 252:80
43. Pothan LA, Thomas S, Groeninckx G (2006) Compos Part A 37:1260
44. Brostow W, Hagg Lobland HE (2010) J Mater Sci 45:242. doi:10.1007/s10853-009-3926-5
45. Brostow W, Kovačević V, Vrsaljko D, Whitworth (2010) J Mater Edu 32:273
46. Brostow W, Hagg Lobland HE (2006) J Mater Res 21:2422
47. Brostow W, Datashvili T, Geodakyan J, Lou J (2011) J Mater Sci 46:2445. doi:10.1007/s10853-010-5091-2